Whole-Brain Layer-fMRI Connectome: An Open Dataset for High-Resolution Functional Brain Mapping

Dr. Claire Dubois[1]*
[1]Institut Pasteur, Neuroimaging Research Unit, Paris, France

Abstract

Background – With the first layer-dependent Vascular-Space Occupancy (VASO) studies in humans in 2014/15, a huge breakthrough has been made. Since then, layer-functional magnetic resonance imaging (fMRI) is an emerging method, permanently challenging cutting edge of technology in the neuroimaging field.

Purpose – Here, we provide an exemplary layer-dependent whole-brain fMRI connectome acquired at ultra-high magnetic field of 7 Tesla (T), coming along with a quality assessment comprising metrics of skew, kurtosis, temporal Signal-to-Noise Ratio (tSNR) and sharpness. This dataset demonstrates consistency and reproducibility of a whole brain layer-fMRI connectome paving the way for novel research questions in the neuroscientific field. The purpose of this dataset is to 1.) characterize the prospects and challenges of whole brain layer-fMRI acquisition sequences in a test-retest setting and 2.) to provide a test bed for developing and benchmarking new layer-dependent analysis tools.

Data Accessibility – This is an initial release of an ongoing study, published in line with the Brian Imaging Data Structure (BIDS) standard on OpenNeuro, a free and open platform for sharing research data. We are happy to share the data via SIEMENS C2P.

Scanning and Acquisition Choices

Scanning at 7 Tesla

Scanning was performed at Scannexus as part of the Maastricht Brain Imaging Centre (MBIC) embedded in the Maastricht University, Maastricht, The Netherlands. VASO and Blood-oxygen-level-dependent (BOLD) contrasts of the whole brain were obtained from one participant at a SIEMENS MAGNETOM 7-Tesla scanner at six days while watching the Human Connectome Project (HCP) audio movie. For information about detailed scanning parameters click here. There is no data available for day 3 due to technical issues at scanning (PCI_RX receiver error). At day 6, respiration and pulse were recorded to provide the required physiological measures for further analysis. Link to physiological recording on Github.

The following sequences were applied:

- mp2rage_iso0.65_iPAT2_angulated (voxel size: 0.65×0.65×0.65 mm)
- mp2rage_iso0.65_iPAT2_angulated_multi_echo
  (voxel size: 0.65×0.65×0.65 mm)
- VASO_151_0.8mm_120sl_noPO (voxel size: 0.8×0.8×0.8 mm)

In the process of data acquisition, choices regarding shimming, flip angle (FA) and registration have been made. Also, a movie was chosen for perceptual stimulation while scanning.

3rd order shimming

At ultra-high field imaging, spectral resolution and SNR can benefit from higher order shimming over linear and second order shimming only. Artefacts are reduced and the main magnetic field B0 is kept as homogenous as possible. We used 3rd order shimming, showing the advantage in the GIF below:

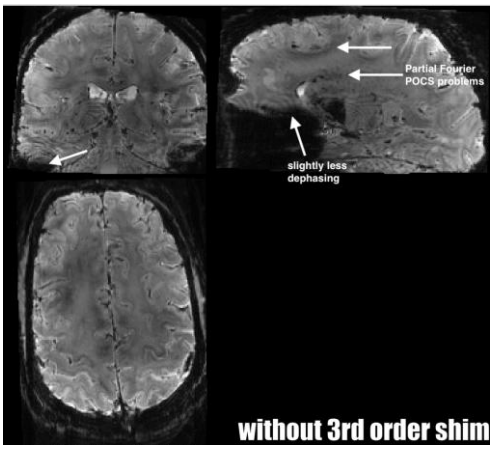

GIF 1. Showing scanning results with and without 3rd order shimming.

Flip Angle Comparison: 6° versus 12°

The initial rotation of the net magnetization (M) caused by the radiofrequency pulse (RF pulse) is crucial for signal intensity and image contrast. Especially at high field strengths it is important to consider a suitable FA. Temporal SNR comparison shows advantage of using a 12° FA. Calculated mean and standard deviation (SD) also suggest the 12° FA (Table 1.)

	BOLD		VASO	
	6° FA	12° FA	6° FA	12° FA
Mean	13	15	11	12
SD	6	7	5	6

Table 1. Calculated mean and SD of tNSR showing a slight advantage of a 12° FA.

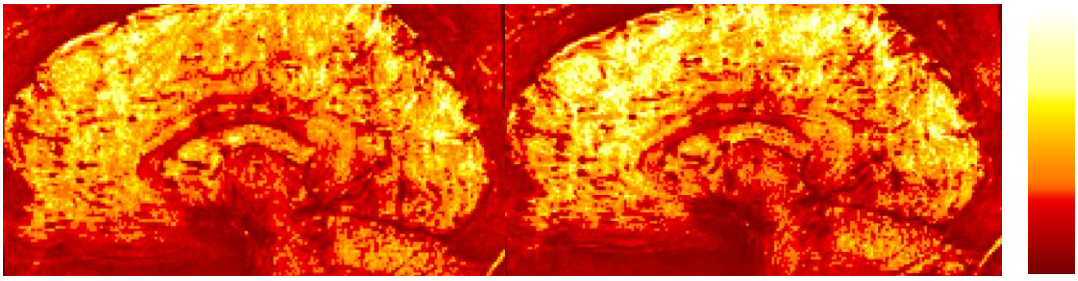

Figure 1. Sagittal view: 6° FA (left) versus 12° FA (right).

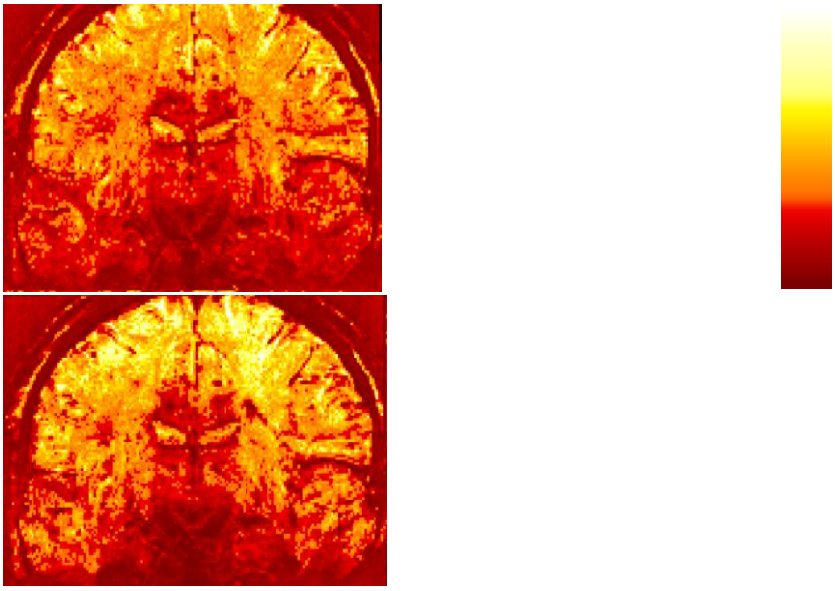

Figure 2. Coronal view: 6° FA (left) versus 12° FA (right).

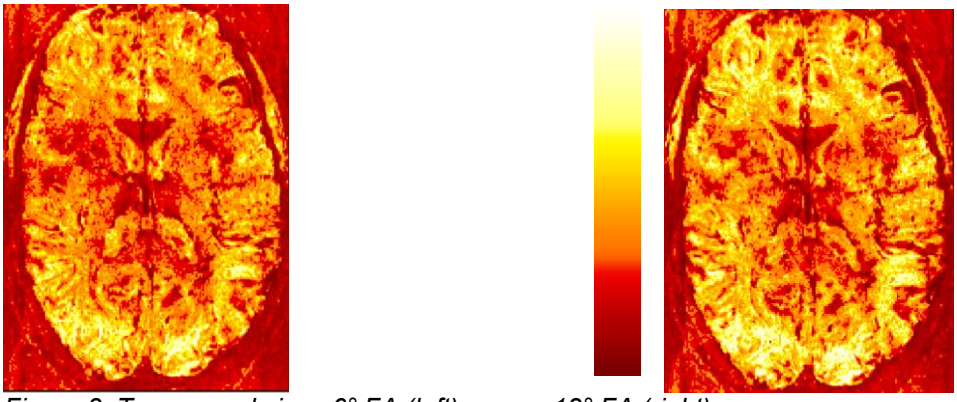

Figure 3. Transversal view: 6° FA (left) versus 12° FA (right).

Registration

Registration was done with Advanced Normalization Tools (ANTS).
Data was averaged across sessions, runs and time points to get a dataset that is as accurate and noise-free as possible.

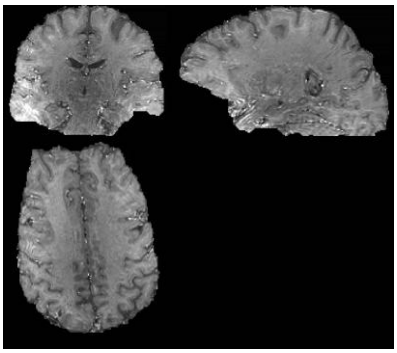

GIF 2. Image Comparison across sessions.

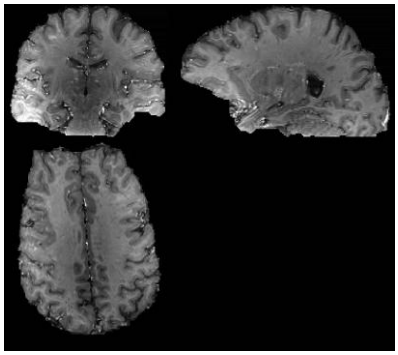

GIF 3. Image Comparison across runs within sessions

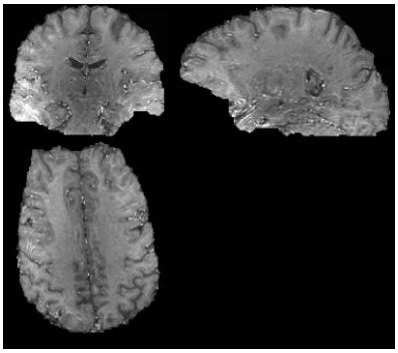

GIF 4. Image Comparison across time points within runs.

This way of registration was chosen based on its superior quality compared to alternative analysis approaches, e.g. with Syn template matching in ANTS or iterative day and session registration.

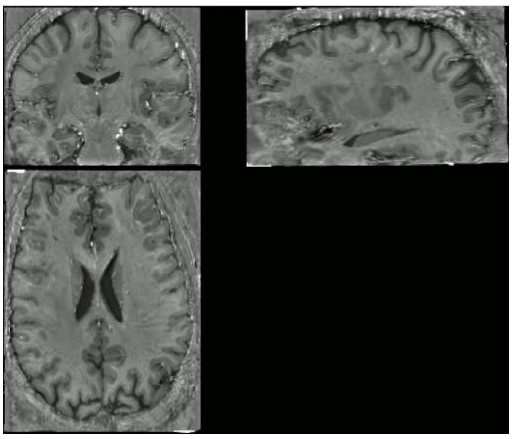

GIF 5. Syn template matching in ANTS showing confusion-affected right hemisphere. Two datasets were matched to one single template.

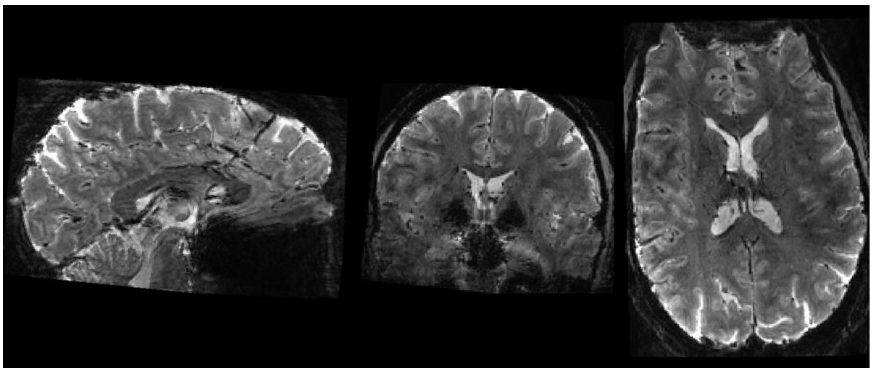

GIF 6. Iterative day and session registration within runs, across runs and sessions.

Movie

For acoustic as well as visual stimulation during scanning, the Human Connectome Project (HCP) audio movie from the Vimeo clip collection (Link to PsychoPy stimulation

and Link to movie file) was presented. The movie consists of four different video clips. Detailed information about time frame and FPS of these clips can be found in Table 2. Each session comprises several runs (movie presented).

Session	Runs
1	2 (6° and 12° FA)
2	4
3	–
4	5
5	5
6	5

Table 2. Overview about sessions and runs (movie presentations).

	Start Frame	End Frame	Total Duration	FPS	URL
Two_Men	*0*	*5858*	*5859*	*25*	http://vimeo.com/17970306
Welcome_To_Bridgeville	*0*	*5320*	*5321*	*23.98*	http://vimeo.com/31318354
Pockets	*0*	*4513*	*4514*	*25*	http://vimeo.com/14216866
Inside_the_Human_Body	*0*	*1530*	*1531*	*25*	http://vimeo.com/24930096
Vimeo_Repeat			*2002*	*23.98*	

Table 3. Detailed information about movie clips. 7T_MOVIE1_CC1

Data Processing

Steps of Data Processing

Repetition Time (TR) as well as resolution is variable across time and contrasts within one run. TR for raw data was 8.9640 seconds, for processed data 4.482 seconds.

Data processing consists of 6 steps: (1) file format conversion, (2) defacing, (3) Motion correction (MOCO), (4) BOLD-correction (BOCO), (5) segmentation and (6) layering. First, raw data in DICOM (*.dcm) format are converted into NIfTI (*.nii) format. Defacing was performed with FreeSurfer (v6.0) (Fischl, 2012). Since the acquired data consist of interleaved VASO and BOLD components, MOCO was performed for both, respectively. For the AFNI/ANTS version of MOCO click here. BOLD correction comprises the division of the blood-nulled image with the not-nulled BOLD image (LAYNII program, v1.6.0, Huber et al., 2020, LN-command: LN_BOCO). For the detailed information about the BOCO click here. Motion correction (MOCO) and BOLD correction (BOCO) were both performed with LAYNII. Segmentation describes the differentiation of grey matter (GM) and white matter (WM), used as a mask for further layering. It is performed automatically and manually, based on the T1-weighted image which was acquired on the first day. Starting with creating a GM mask with Statistical Parametric Mapping (SPM, Ashburner, 2012) and BrainVoyager (Goebel, 2012), followed by manual segmentation of GM and WM in ITK.SNAP.

Figure 4. Automatically generated GM mask.

Figure 5. Manually corrected GM mask.

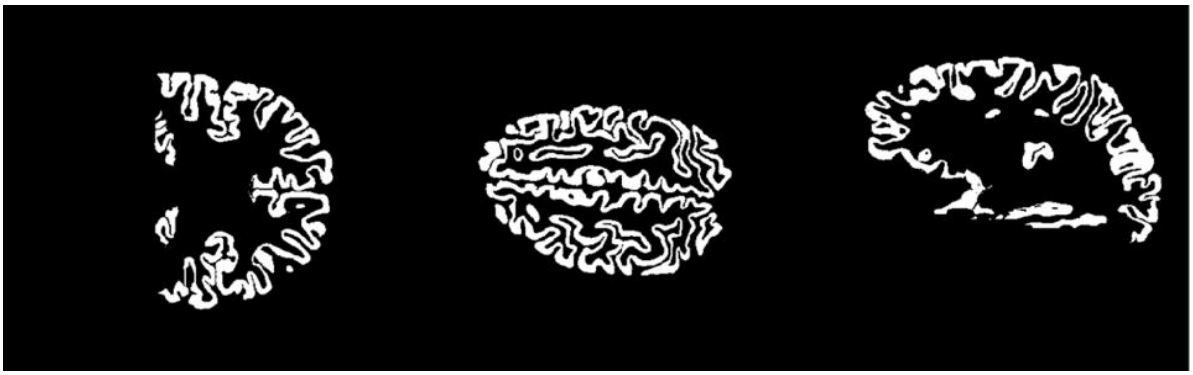

Figure 6. Resulting rim.file.

Last step of the analysis pipeline is defining cortical layers in LAYNII. These can be used for further layer-dependent functional activity analyses. Seven layers were defined. Later, for activation analysis, only five of them were extracted due to their thickness.

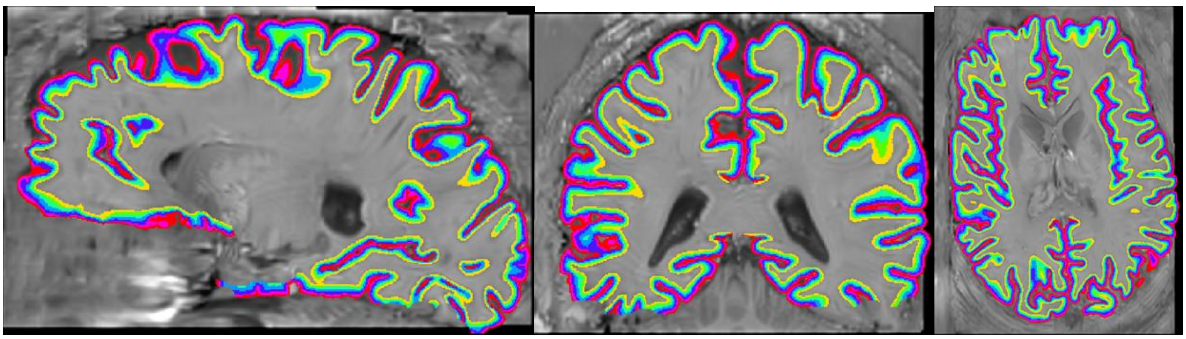

Figure 7. Defined layers. Color coding from CSF to cortical surface: yellow, green, light blue, dark blue, red and pink.

Quality Assessment

Quality Assessment for Layer fMRI Time Series

Quality assessment (QA) provides several tools to check reliability of obtained MRI data. QA measures include mean, tSNR, skewness, kurtosis and sharpness and were performed in LAYNII. QA metrics were calculated and interpreted based on “Quality assurance measures for layer-fMRI time series : How to perform them in LAYNII”, Link. Data: session 6 run 5 (ses-06_run-05)

Mean

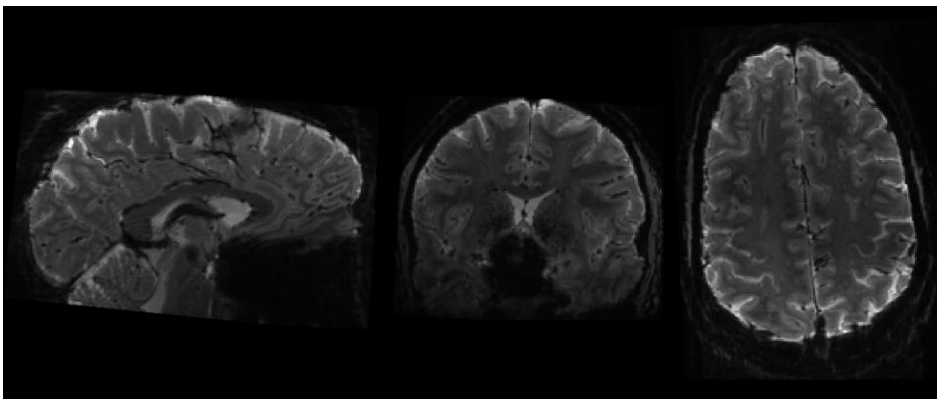

Figure 8. Mean of signal. The typical brain structures can be easily identified.

Temporal Signal-to-Noise Ratio (tSNR)

A commonly used quality measure for MRI data is the temporal Signal-to-Noise Ratio (tSNR). It is defined as the ratio of signal and noise of the time series. The higher the ratio, the better data quality, meaning less noise and more actual signal.

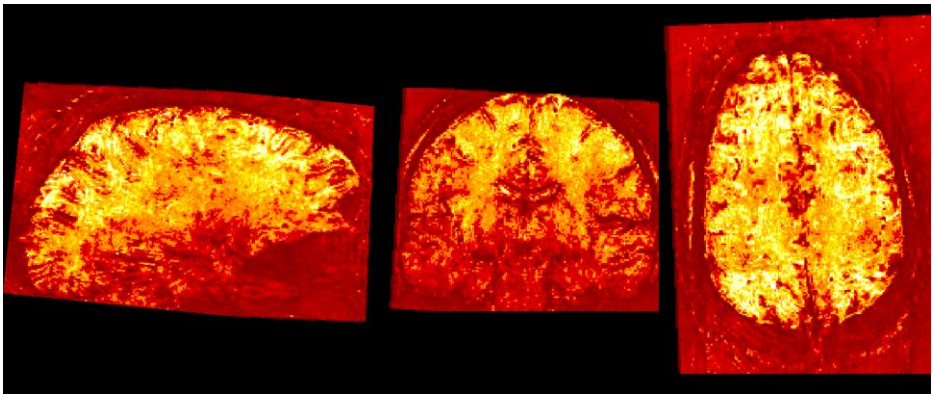

Figure 9. Temporal SNR values for the whole brain. View from sagittal, coronal and transversal (from left to the right).

Skewness and Kurtosis

Especially layer fMRI suffers from uncontrollable noise of different sources. Therefore, assumed Gaussian noise distribution should be checked. Both metrices, skewness and kurtosis, confirm Gaussian distribution in this dataset.

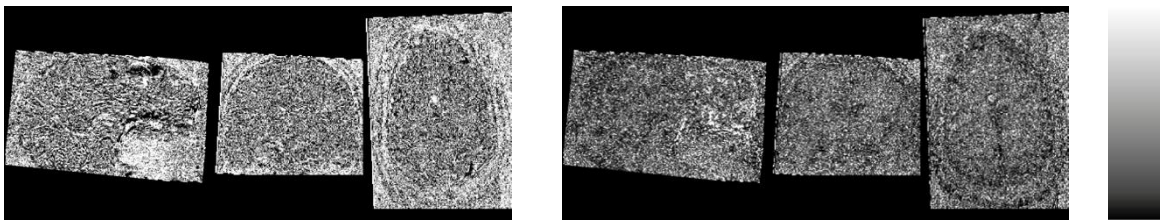

Figure 10 a + b. Both measures do not strongly show geometrical structures. Most of the brain is dominated from Gaussian noise. Only the area above the nasal cavities indicate non-Gaussian noise.

Sharpness–Smoothness for VASO and BOLD

(Nichols T, FMRIB technical report TR08TNI, 2008)

VASO: FWHMvoxel [x = read, y = phase, z = segment] 1.1973 1.46951 1.00693

BOLD: FWHMvoxel [x = read, y = phase, z = segment] 1.14864 1.47221 1.02471

In read direction and segment direction, sharpness is very close to the nominal resolution. Only in the phase encoding direction, the expected T2*-blurring results in wider point spared functions and corresponding blurring.

Functional Sensitivity

Functional activation profiles during movie presentation are shown for the Sulcus calcarinus, Sulcus intraparietalis and Brodmann Area 42.

Sulcus calcarinus

The sulcus calcarinus is a deep sulcus in the medial part of the occipital lobe, supplied by the calcarine branch of the medial occipital artery. The sulcus can be distinguished into a superior bank called “cuneus” and an inferior bank named lingual gyrus. Since the sulcus calcarinus is embedded in the primary visual cortex (V1), it receives visual input from the retina according retinotopic mapping.

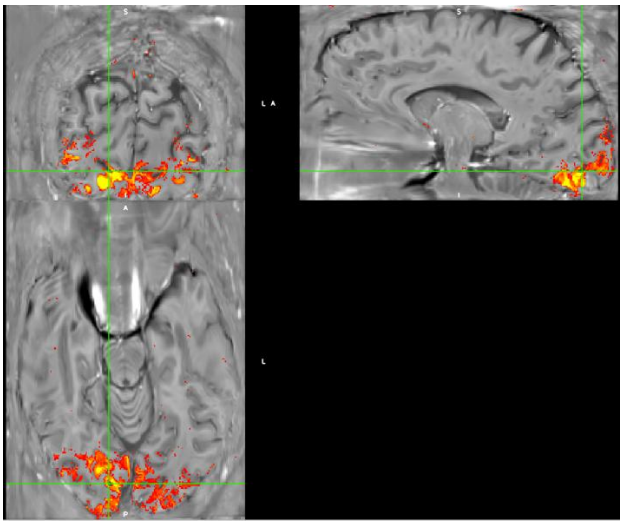

Figure 11a. Activation profile during movie watching. Increased activation shown in the V1, especially in the Sulcus calcarinus.

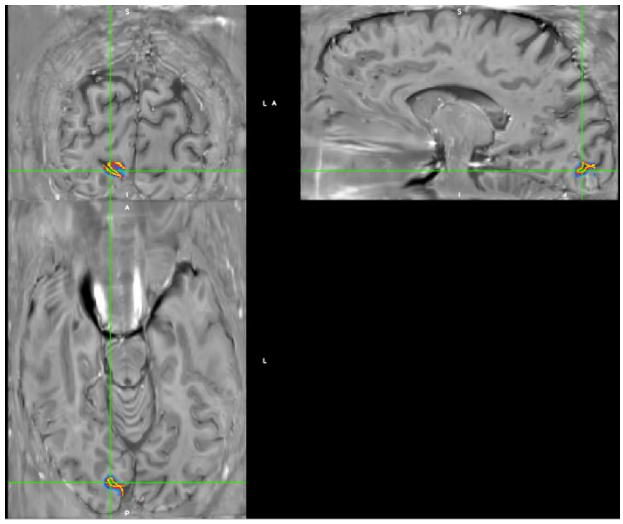

Figure 11b. Representation of layers of the Sulcus calcarinus during movie watching.

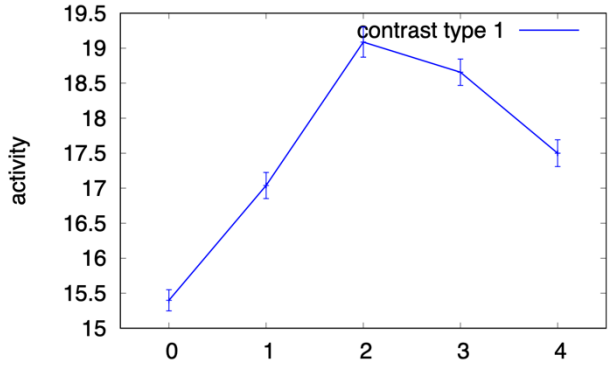

Figure 11c. Activation profile of 5 different cortical layers of the Suclus calcarinus (x-axis). X-Axis representing cortical depth from white matter (0, left) to CSF (4, right) during movie watching. Peak activation shown in granular layers.

Sulcus intraparietalis

The Sulcus intraparietalis (IPS) is located at the lateral surface of the parietal lob, dividing it horizontally into two parts. Besides other functions, the Sulcus intraparietalis is involved in visual attention as well as viso-spacial working memory.

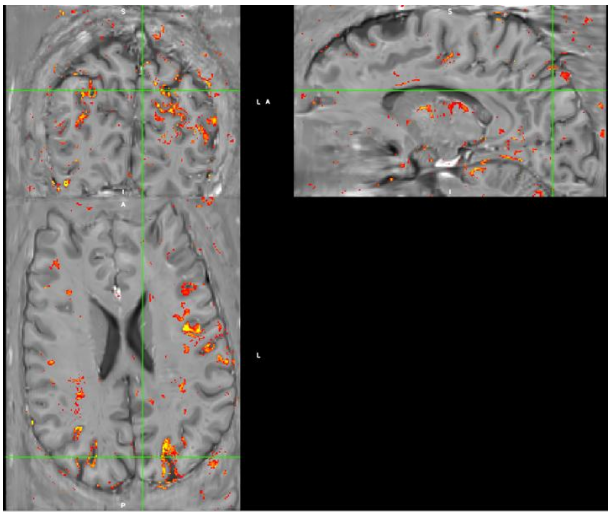

Figure 12a. Activation profile during movie watching. Increased activation shown in the parietal cortex, especially in the Sulcus

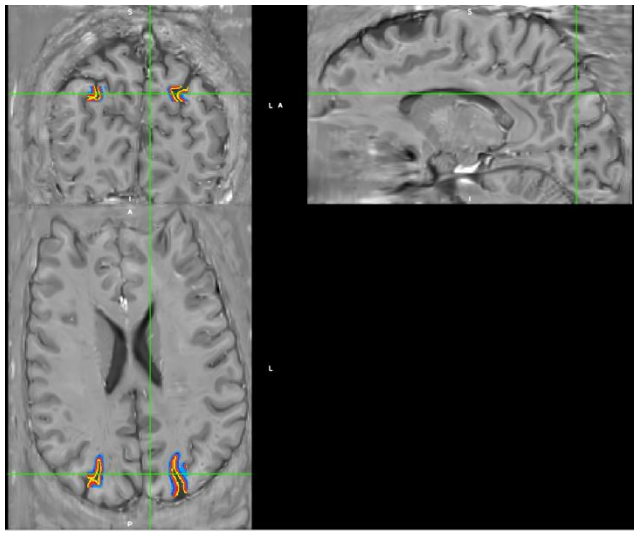

Figure 12b. Representation of layers of the Sulcus intraparietalis during movie watching.

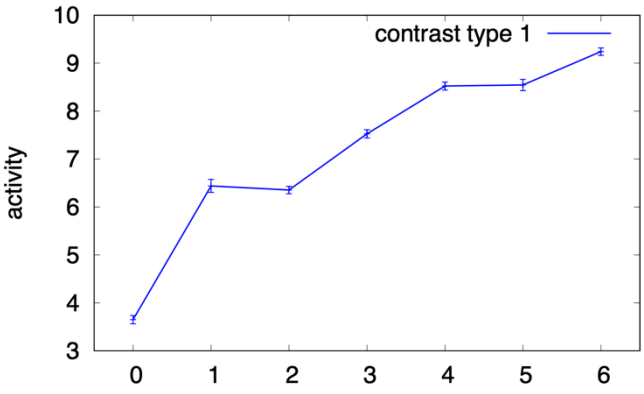

Figure 12c. Activation profile of 5 different cortical layers of the Sulcus intraparietalis (x-axis). X-Axis representing cortical depth from white matter (0, left) to CSF (4, right) during movie watching. Activation increases towards the cortical surface.

Brodmann Area 42

As part of the primary auditory cortex receiving auditory information from the thalamus. According to its tonotopic organization regarding frequencies, it is known to be involved in processing of pitch and loudness of sounds.

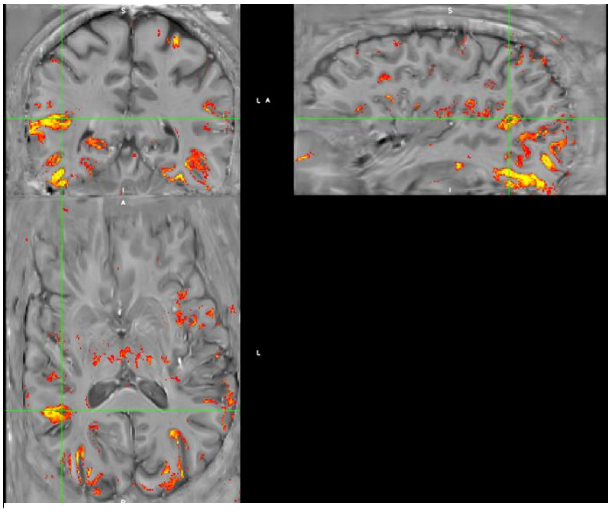

Figure 13a. Activation profile during movie watching. Increased activation shown in the auditory cortex, especially in the Brodmann Area

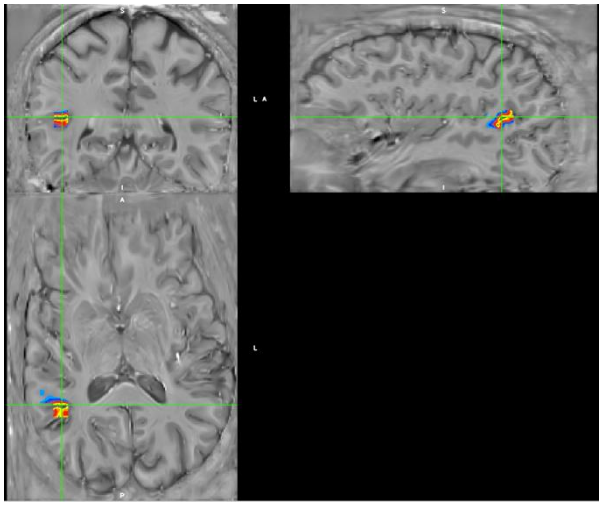

Figure 13b. Representation of layers of the Brodmann Area 42 during movie watching.

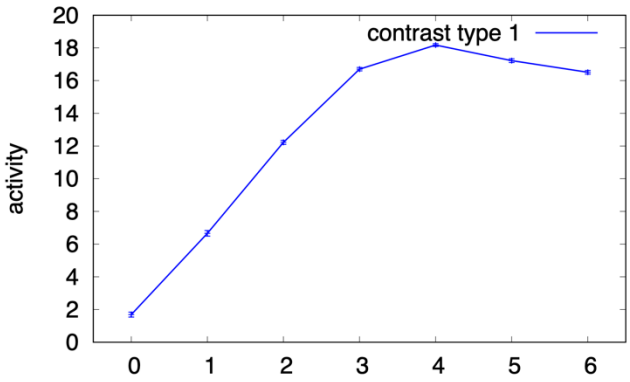

Figure 13c. Activation profile of 5 different cortical layers of the Brodmann Area 42 (x-axis). X-Axis representing cortical depth from white matter (0, left) to CSF (4, right) during movie watching. Activation is dominated from supragranular and granular layers.